JOURNAL OF MATERIALS SCIENCE 30 (1995) 459–464

High T_C dual phase Ag–$YBa_2Cu_3O_{7-x}$ composites prepared by selective laser sintering and infiltration

MUKESH K. AGARWALA, D. L. BOURELL, A. MANTHIRAM, B. R. BIRMINGHAM, H. L. MARCUS
Center For Materials Science and Engineering, The University of Texas at Austin, Austin, Texas 78712, USA

Bulk porous samples of $YBa_2Cu_3O_{7-x}$ were made from powders by selective laser sintering, a near-net-shape forming technology requiring no part-specific tooling. The porous parts were densified by infiltrating silver into the pores, resulting in a dense, dual-phase superconducting composite. The laser-processing parameters were varied to obtain the optimum microstructure. The laser-sintered parts required oxygen annealing after infiltration to restore the orthorhombic, superconducting structure. X-ray diffraction (XRD) and T_c measurements indicated that some impurity phases were present in samples processed under aggressive laser conditions.

1. Introduction

Since the discovery of high T_c ceramic superconductors [1, 2] much work has been devoted to their development for practical applications. Considerable success has been achieved in the area of thin films [3]. However, prototype applications in bulk form are still being investigated. The major obstacles to making practical bulk shapes from these materials are their inferior current-carrying capacity in the bulk form and their poor mechanical properties. These two factors have been investigated widely, but with limited success. High-critical-current-density parts have been made by melt texturing [4], which results in the oriented grained structures which are necessary for high critical current densities. However, bulk samples prepared by such techniques have poor mechanical and fracture properties. Attempts at improving the mechanical properties have been made by incorporating a ductile phase such as silver in the $YBa_2Cu_3O_{7-x}$ matrix [5–7]. This has been done in fabrication techniques such as cold pressing and sintering [5], tape casting [5] and powder-in-tube rolling [8]. But these fabrication techniques do not result in the oriented-grained structure that is necessary for high critical current density.

In this study we report on a technique for making rapid prototype bulk parts of Ag–$YBa_2Cu_3O_{7-x}$ which have the potential of carrying high current densities. In this study porous preforms of $YBa_2Cu_3O_{7-x}$ were formed in the required shape and then infiltrated with silver to create a dense, dual-phase, composite part. Selective laser sintering (SLS) offers the possibility of forming such net-shaped porous preforms of ceramics.

SLS is a solid-freeform fabrication (SFF) technique by which near-net-shaped parts can be made without part-specific tooling [9]. SLS has been used successfully to fabricate prototype parts and preforms with polymers, ceramics and metals [10, 11]. In this process a computer-controlled laser beam is used to sinter selected areas of a powder bed. An additional layer of powder is spread on the previously selectively laser-sintered layer, and the process is then repeated by scanning the laser beam across the fresh powder layer. This process continues until a three-dimensional sintered part is built up layer by layer. At the end of the process, the sintered part is removed from the surrounding loose powder.

SLS is a pressureless sintering process which usually involves a liquid phase [12]. Atomic diffusion in the liquid phase is faster than in solid-state processes. The liquid phase can also assist in particle rearrangement due to reduced interparticle friction. A partial liquid phase is formed and solidified as the laser beam is scanned across the powder bed in a directional fashion. Such directional formation and solidification of the liquid phase can result in an oriented, grained structure. Since $YBa_2Cu_3O_{7-x}$ melts incongruently [13, 14], it is possible to form a partial liquid phase by careful control of the laser power density to induce interphase melting. Other laser-processing parameters which affect the microstructure and hence the properties include the laser scan speed, the scan spacing and the layer thickness. These laser-processing parameters have been studied extensively for various ceramic, metals and polymer systems [11, 12]. By careful manipulation of these parameters, and of the powder characteristics such as the particle size, a desirable microstructure with optimum properties can be obtained.

In this study, an attempt was made to produce bulk parts of $YBa_2Cu_3O_{7-x}$ by selectively laser sintering a preform and then infiltrating it with a ductile silver phase to obtain a dense, dual-phase, superconducting composite.

0022–2461

2. Experimental procedure

$YBa_2Cu_3O_{7-x}$ precursor powders were prepared using the citrate sol–gel technique [15]. The precursor powders were calcined at 900 °C in oxygen for 10 h. Following calcination, the powders were oxygen annealed at 600 °C for 6 h resulting in powders with an average particle size of 100 nm. An SLS workstation system developed by Birmingham *et al.* [16] (shown schematically in Fig. 1) was used to carry out the sintering. The basic system operation procedure is outlined here.

1. The system starts with the traversing roller to the far left, with the powder-feed piston fully retracted with its chamber loaded with powder, and with the powder-accept piston in the fully extended position.
2. The system is evacuated and then filled with the desired gas(es).
3. Powder is made available to the roller by raising the powder-feed piston by an incremental amount.
4. The powder-spreading roller is traversed across the stage and then back, spreading the powder into a thin layer on the stage.
5. The laser is then scanned, selectively sintering an area of the powder above the powder-accept piston.
6. The powder-accept piston is lowered by an incremental amount which is dictated by the desired layer thickness.
7. Powder is again made available to the roller by raising the powder-feed piston.
8. The powder-spreading roller is traversed across the stage, spreading the powder over the powder-accept piston and across the previously sintered area.
9. The laser is then scanned, sintering the second layer.
10. Steps 3 to 9 are repeated, building up the three-dimensional part layer by layer.

All SLS processing was carried out in air at room temperature. A 25 W CO_2 laser was used with a beam diameter of 700 μm . Three-dimensional square parts with 8 mm long sides were made layer by layer to final thicknesses ranging from 1 to 3 mm. The laser power density was varied from 500 W cm^{-2} to 1300 W cm^{-2}. Laser scan speeds of 1 to 3 mm s^{-1} were employed. The scan spacing was kept constant at 100 μm for all runs. The layer thickness was varied from 250 to 150 μm. The initial layers were thicker (200–250 μm), to avoid displacement of the previously sintered layers by the roller action during the spreading of powder to lay fresh layers for sintering. As more layers are sintered, the overall thickness of the sample increases, making the displacement of the structure, by roller action, difficult. This makes it possible to reduce the layer thickness. Therefore, the layer thickness was gradually reduced to 150 μm. The final thickness of the sample was thus controlled by the layer thickness and by the number of layers.

The porous parts obtained by SLS were infiltrated with silver to fill up the pores and to provide a reinforcing ductile phase. Silver infiltration was accomplished by placing the samples in an alumina boat with sufficient silver powder (0.7–1.3 μm) on top of the samples [17]. The boat with the sample and the infilterant was heated in a vertical tube furnace at 970 °C in air for 10 to 30 min. The process was continuously monitored visually to allow melting of silver and its infiltration, by a capillary effect, into the porous $YBa_2Cu_3O_{7-x}$ samples while avoiding any significant melting of the $YBa_2Cu_3O_{7-x}$ sample, which would have resulted in a loss of shape. Table I lists the various laser parameters used for samples with and without silver infiltration.

The SLS porous parts and the silver-infiltrated

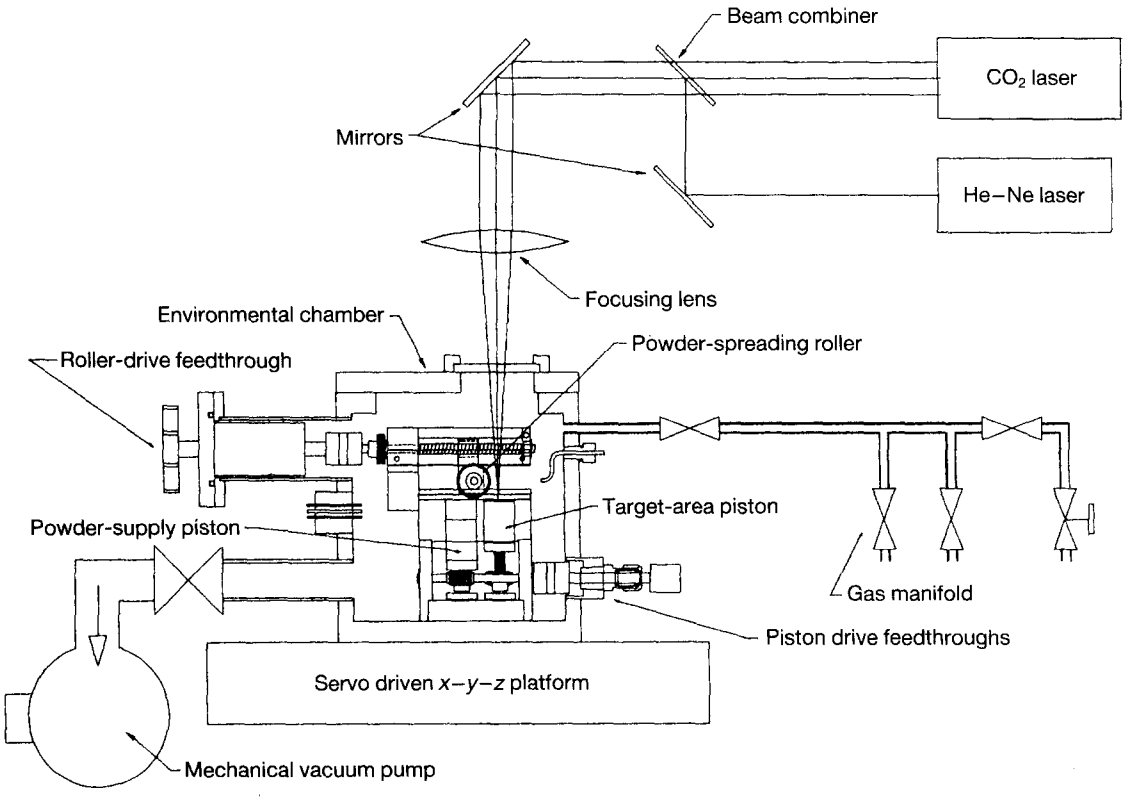

Figure 1 An SLS workstation.

TABLE I The SLS processing parameters and post-SLS processes

Sample	Laser power ($W cm^{-2}$)	Speed ($mm s^{-1}$)	Silver infiltration (970 °C)	O_2 annealing temperature (930 °C)
A	600	1.0	No	Yes
B	750	1.0	No	Yes
C	1000	1.0	No	Yes
D	1300	1.0	No	Yes
E	750	1.5	No	Yes
F	750	2.0	No	Yes
G	600	1.0	Yes	Yes
H	750	1.0	Yes	Yes
I	1000	1.0	Yes	Yes

dense parts were annealed at 930 °C for 8–10 h in flowing oxygen and then they were slowly cooled in flowing oxygen. Structural phases of the samples were investigated at each stage of processing by X-ray diffraction (XRD). Critical transition temperatures were measured by a superconducting-quantum-interference-device (SQUID) magnetometer. The samples were weighed before and after the silver infiltration to determine the volume fraction of the porosity at each stage and to find the degree of silver infiltration. A Micromeritics Accupyc 1330 pycnometer was used to determine the degree of open versus closed porosity. The sample microstructures and the distribution of silver were studied by scanning electron microscopy (SEM).

3. Results and discussion

The XRD pattern of the starting superconducting powder, prepared by a citrate sol–gel technique was identified as a single-phase composition of orthorhombic $YBa_2Cu_3O_{7-x}$. Signals of any impurity phases were not detectable (Fig. 2a).

The partial liquid phase, which is necessary for SLS, was created by using a sufficiently high laser power density to produce a temperature above the peritectic decomposition temperature of $YBa_2Cu_3O_{7-x}$, producing Y_2BaCuO_5 and a liquid phase, L, according to the reaction [13, 18]

$$YBa_2Cu_3O_{7-x} \longrightarrow Y_2BaCuO_5 + L$$

The amount of the liquid phase, L, which formed depended on the degree of peritectic superheating.

As shown in Fig. 2b, the XRD patterns of SLS parts did not exhibit significant crystallinity, for any of the laser processing parameters; but these patterns did indicate a breakdown in the $YBa_2Cu_3O_{7-x}$ structural phase into various phases, such as Y_2BaCuO_5, $BaCuO_{2-x}$ and $BaCu_2O_2$. The existence of metastable, noncrystalline phases is expected after SLS, because of the rapid melting and solidification of the ceramic $YBa_2Cu_3O_{7-x}$ in the process. However, following SLS, the crystallinity and the superconducting phase, $YBa_2Cu_3O_{7-x}$ were restored in the SLS parts by oxygen annealing and slow, controlled cooling (see Fig. 2c and d). Small amounts of the impurity phases of Y_2BaCuO_5, $BaCu_2O_2$ and $BaCuO_{2-x}$ were still found in the samples. As shown in Fig. 2c and 2d, the samples processed at high laser power densities ($> 1000 W cm^{-2}$) contained higher degrees of non superconducting phases even after oxygen annealing. Higher laser power densities raise the powder temperature sufficiently to form large amounts of the liquid phase, L, and very small amounts, or none of the solid phase, Y_2BaCuO_5. Such large amounts of the liquid phase leads to significant chemical segregation and complete breakdown of the $YBa_2Cu_3O_{7-x}$ structure. Such severe breakdown in the structure makes it more difficult for the stoichiometric, orthorhombic structure to be regained completely during oxygen annealing at 930 °C for 8–10 h, thus leaving residual impurity phases. Lower laser power densities ($< 1000 W cm^{-2}$) result in partial melting of the powders, according to the above mentioned peritectic reaction, leading to partial breakdown of the $YBa_2Cu_3O_{7-x}$ structure and to less chemical segregation. Therefore a nearly pure phase of $YBa_2Cu_3O_{7-x}$ is easily regained by simple oxygen annealing, when the laser power density produces only a partial melting of the $YBa_2Cu_3O_{7-x}$ powders.

Localized heating of the powder bed results in a temperature gradient along the scan line during SLS. If the temperature gradient is large, residual stresses appear in the sample which can lead to macrocracks and debonding of the layers. As shown in Fig. 3a and b, the surface and the cross-section of a laser-sintered $YBa_2Cu_3O_{7-x}$ part showed some macrocracks but there was no significant debonding of layers. High laser power densities and low scan speeds, which tend to aggravate this problem, also produced no significant debonding of the layers in $YBa_2Cu_3O_{7-x}$.

The bulk density of various SLS metal and ceramic parts has been found to be affected by the laser processing parameters. In this study, the bulk density of laser-sintered $YBa_2Cu_3O_{7-x}$ parts varied from 55 to 75% of the theoretical density as the laser power density increased from 500 $W cm^{-2}$ to 1300 $W cm^{-2}$ at a constant scan speed of 1 $mm s^{-1}$ (Fig. 4). The bulk density also varied from 55 to 65% as the scan speed decreased from 2 to 1 $mm s^{-1}$ at a constant power density of 700 $W cm^{-2}$ (Fig. 5). Reduced layer thicknesses were found to improve the bulk density significantly. However, thick layers had to be used in the initial building up of the structure to prevent displacement of the layers by the traversing roller. The density of the $YBa_2Cu_3O_{7-x}$ samples was also measured using a helium-gas pycnometer. Using the theoretical density of $YBa_2Cu_3O_{7-x}$ and the densities determined by the pycnometer, it was concluded that the porous,

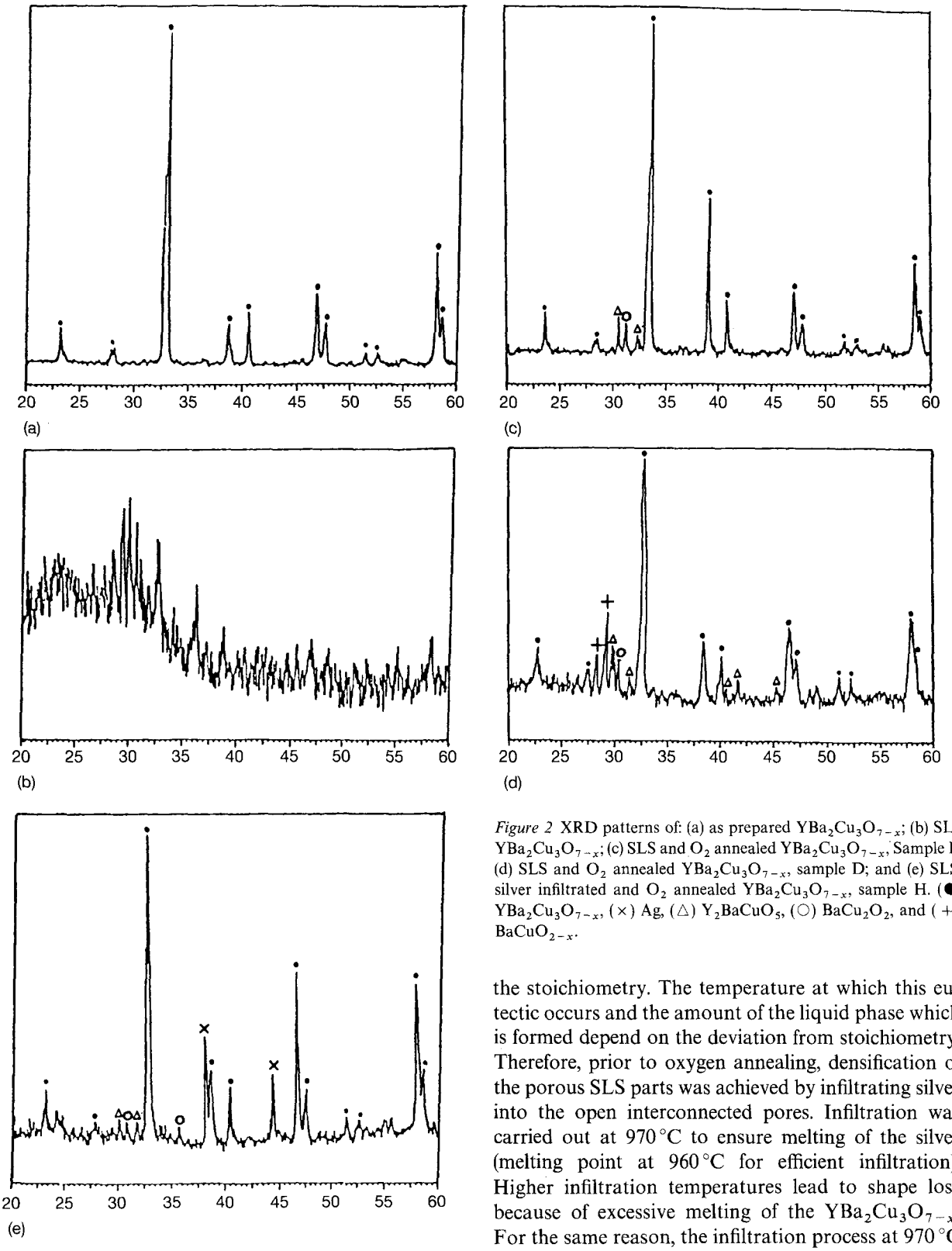

Figure 2 XRD patterns of: (a) as prepared $YBa_2Cu_3O_{7-x}$; (b) SLS $YBa_2Cu_3O_{7-x}$; (c) SLS and O_2 annealed $YBa_2Cu_3O_{7-x}$, Sample B, (d) SLS and O_2 annealed $YBa_2Cu_3O_{7-x}$, sample D; and (e) SLS, silver infiltrated and O_2 annealed $YBa_2Cu_3O_{7-x}$, sample H. (●) $YBa_2Cu_3O_{7-x}$, (×) Ag, (△) Y_2BaCuO_5, (○) $BaCu_2O_2$, and (+) $BaCuO_{2-x}$.

SLS parts had predominantly open, interconnected porosities with a closed porosity of only 1–2%.

Oxygen annealing of the SLS parts at 930 °C for 8–10 h restored the desired orthorhombic $YBa_2Cu_3O_{7-x}$ structural phase, but it did not improve the bulk density of the samples significantly. Higher annealing temperatures (> 940 °C), for similar time periods, increased the bulk densities moderately but not significantly; this had a cost of a partial or a complete loss of shape. Partial liquid-phase formation can occur in $YBa_2Cu_3O_{7-x}$ above 900 °C by a eutectic reaction arising from CuO and/or BaO enrichment in the stoichiometry. The temperature at which this eutectic occurs and the amount of the liquid phase which is formed depend on the deviation from stoichiometry. Therefore, prior to oxygen annealing, densification of the porous SLS parts was achieved by infiltrating silver into the open interconnected pores. Infiltration was carried out at 970 °C to ensure melting of the silver (melting point at 960 °C for efficient infiltration). Higher infiltration temperatures lead to shape loss because of excessive melting of the $YBa_2Cu_3O_{7-x}$. For the same reason, the infiltration process at 970 °C was continuously monitored, and the process was stopped in 10–30 min when all the silver on top of the $YBa_2Cu_3O_{7-x}$ samples had melted and infiltrated into the pores. Keeping the time periods for the infiltration short prevented any loss of shape, even though the infiltration temperature (970 °C) was above the eutectic temperature. This is probably because of the relatively small amount of the liquid phase which formed. However, such short infiltration time periods did not result in restoration of the $YBa_2Cu_3O_{7-x}$ phase in the parts. Therefore, following SLS and silver infiltration, the samples were oxygen annealed at 930 °C for 8–10 h.

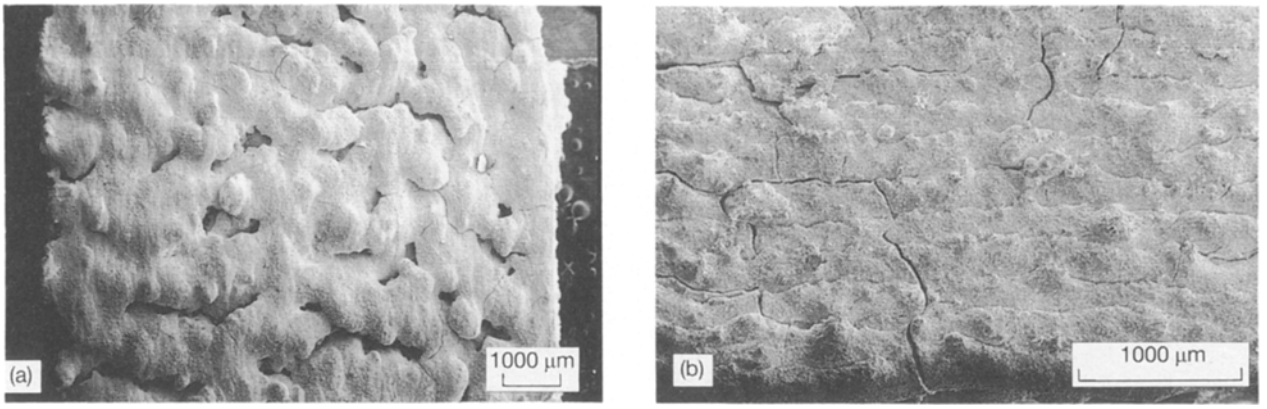

Figure 3 SEM micrographs of an SLS $YBa_2Cu_3O_{7-x}$ sample: (a) the surface, and (b) the cross-section.

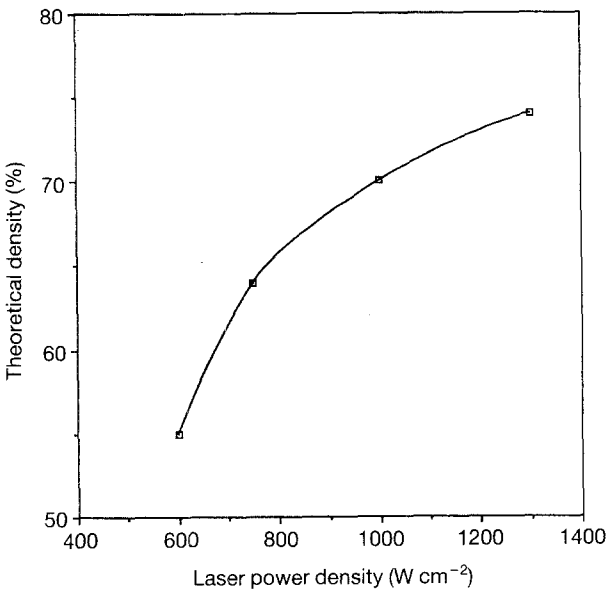

Figure 4 The bulk density of SLS parts as a function of the laser power density.

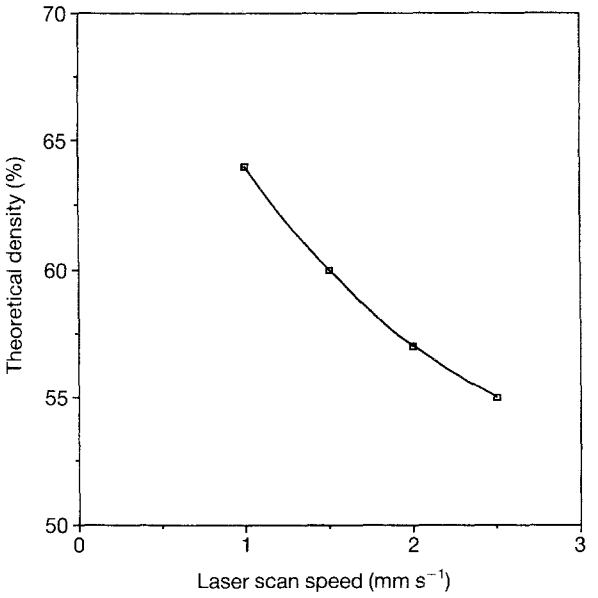

Figure 5 The bulk density as a function of the laser scan speed.

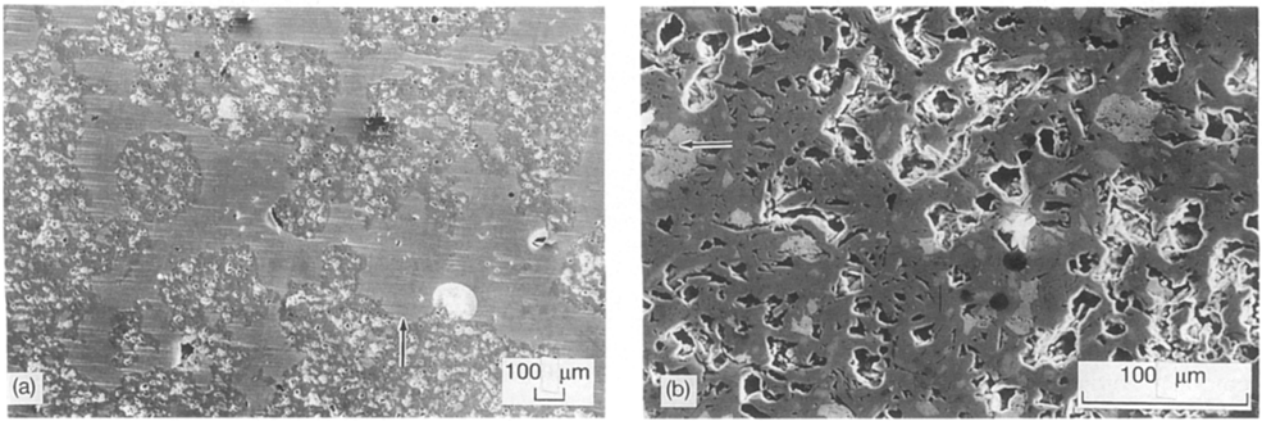

Figure 6 SEM micrographs of SLS and silver infiltrated $YBa_2Cu_3O_{7-x}$ samples.

As shown in Fig. 6, infiltration occurred throughout the cross-section of the sample. Large, continuous pores were infiltrated completely by the silver, whereas the infiltration into the micropores was limited. This is probably because of the relatively high viscosity resulting from the small superheating of the molten silver, which hindered infiltration into the micropores. The bulk density of the samples after the silver infiltration was 85–90%. The volume fraction of the silver in the samples varied from 30 to 45%, depending on the volume fraction of the pores before infiltration and depending on the time of infiltration.

SQUID magnetometer T_c measurements for different samples are shown in Fig. 7. The value of T_c (onset), under field-cooled conditions for all the samples, was approximately 88–90 K. There is a slight broadening of the transition width for samples processed under aggressive laser conditions and for the

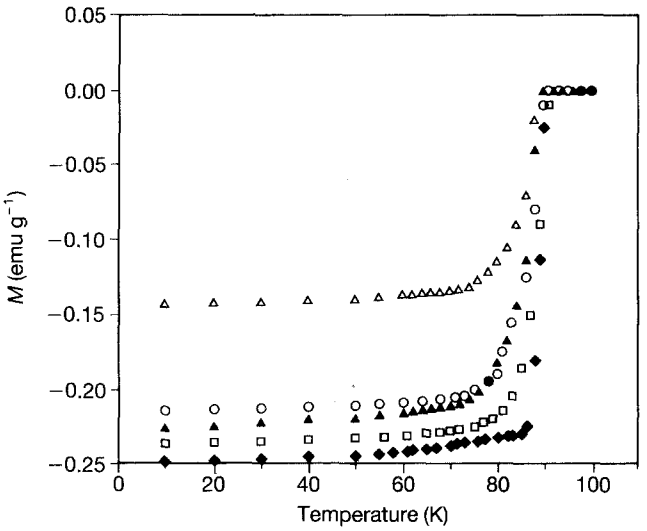

Figure 7 Field-cooled (20 gauss) magnetization data as a function of temperature for ◆ as prepared $YBa_2Cu_3O_{7-x}$ powders; (□) low-laser power-SLS and O_2-annealed $YBa_2Cu_3O_{7-x}$; sample B; (○) high-laser power-SLS and O_2-annealed $YBa_2Cu_3O_{7-x}$, sample D; (△) low-laser power-SLS, silver infiltrated and O_2-annealed $YBa_2Cu_3O_{7-x}$, sample H; and (▲) the data for the previous curve divided by (1 minus the weight fraction of Ag).

silver-infiltrated parts. Transition-width broadening is usually associated with the presence of bulk second phases. Parts processed under aggressive laser conditions have some impurity second phase, as evidenced from XRD, which results in transition-width broadening. Silver-infiltrated parts have continuous networks of silver as a second phase which causes the broadening. However, in all cases, T_c^{zero} occurs well above the liquid-nitrogen temperature of 77 K. Comparison of diamagnetic signals of samples processed by SLS and oxygen annealing (See Fig. 7: □, ○) with that of as prepared $YBa_2Cu_3O_{7-x}$ powders (Fig. 7:◆) reveals that SLS followed by oxygen annealing does not result in any significant reduction in the fraction of the superconducting phase. This is in good agreement with the XRD data, which show very small quantities of non-superconducting phases after SLS and oxygen annealing. Similarly, a comparison of the as received data and weight-fraction-compensated silver infiltrated data, (▲) in Fig. 7 shows that silver infiltration in conjunction with SLS does not result in any significant fraction of non-superconducting phases. This is also in good agreement with the XRD data, and it indicates that during silver infiltration, no chemical reaction occurs which would result in any non-superconducting phases. This has also been observed in other composite studies for Ag–$YBa_2Cu_3O_{7-x}$ [8, 19].

4. Conclusions

Fine powders of superconducting $YBa_2Cu_3O_{7-x}$ were successfully fabricated into bulk, porous shapes by SLS, and they were subsequently densified by silver infiltration at 970 °C. The relationships between the laser-processing parameters and the resulting physical and superconducting properties can be summarized as follows.

1. The bulk density of SLS $YBa_2Cu_3O_{7-x}$ parts improves with increased laser power densities, with reduced scan speeds and with reduced layer thicknesses.

2. Oxygen annealing restored a nearly phase pure orthorhombic $YBa_2Cu_3O_{7-x}$ structure in parts processed under lower laser power densities ($< 1000\ W\ cm^{-2}$).

3. Silver was found to infiltrate successfully into large, continuous pores, improving the bulk density, whereas micropores were only partially infiltrated.

4. T_c onset for SLS parts and silver-infiltrated parts was 88–90 K.

5. Broad transition widths were observed for parts processed under high laser powers and for those infiltrated with silver.

Acknowledgements

The authors would like to thank Laura Henderson for her support and help in the use of the Micromeritics Accupyc 1330 pycnometer. Financial support by NSF grant number DMR 9109080 for the acquisition of a SQUID magnetometer and ONR Grant N00014-92-J-1514 is gratefully acknowledged.

References

1. J. G. BEDNORZ and K. A. MULLER, *Z. Phys. B: Condens. Mater.* **64,** (1986) 189.
2. M. K. WU, J. R. ASBURN, C. J. TORNG, D. H. HOR, R. L. MENG, L. GAO. Z. J. HUANG. Y. Q. WANG and C. W. CHU, *Phys. Rev. Lett.* **58,** (1987) 908.
3. T. VENKATESAN, X. D. WU, B. DUTTA, A. INAM, M. S. HEGDE, D. M. HWANG, C. C. CHANG, L. NAZAR and B. WILKINS, *Appl. Phys. Lett.* **54** (1989) 6.
4. S. JIN, T. H. TIEFEL, R. C. SHERWOOD, R. B. VAN DOVER, M. E. DAVIS, G. W. KAMMLOTT and R. A. FASTNACHT, *Phys. Rev. B.* **37** (1988) 7850.
5. J. P. SINGH, H. J. LEU, R. B. POEPPEL, E. VAN VOORHEES, G. T. GOUDEY, K. WINSLEY and D. SHI, *J. Appl. Phys.* **66**(7) (1989) 3154.
6. L. S. YEOU and K. W. WHITE, *J. Mater. Res.* **7**(1) 1 (1992).
7. M. K. AGARWALA, Doctoral dissertation, University of Texas, Austin TX USA, 1994.
8. S. SEN, I. CHEN, C. H. CHEN and D. M. STEFANESCU, *Appl. Phys. Lett.* **54**(8) (1989) 766.
9. H. L. MARCUS, J. J. BEAMEN, J. W. BARLOW and D. L. BOURELL, *Ceramic Bulletin* **69**(6) (1990) 1030.
10. D. L. BOURELL, H. L. MARCUS, J. W. BARLOW and J. J. BEAMEN, *Int. J. Powder. Met.* **28**(4) (1992) 369.
11. H. L. MARCUS, J. J. BEAMEN, J. W. BARLOW, D. L. BOURELL, and R. H. CRAWFORD (eds), Proceedings of the Solid Freeform Fabrication Symposium, 1991, Aug. 12–14, 1991, The University of Texas at Austin, Austin, Texas.
12. G. ZONG, Y. WU, N. TRAN, I. LEE, D. L. BOURELL, J. J. BEAMEN and H. L. MARCUS (eds), "Direct Laser Sintering of High Temperature Materials", Proceedings of the SFF Symposium, Austin, Texas, Aug. 3–5, 1992.
13. K. OKA, K. NAKANE, M. ITO, M. SAITO and H. UNOKI, *Jpn. J. Appl. Phys.* **27**(6) (1988) L1065.
14. N. NEVRIVA, P. HOLBA, S. DURCOK, D. ZEMANOVA, E. POLLERT and A. TRISK, *Physica C*, **157** (1989) 334.
15. M. KAKIHANA, L. BORJESSON, S. ERIKSON, P. SVEDLINDH and P. NORLING, *ibid.* **162** (1989) 931.
16. B. R. BIRMINGHAM, J. V. TOMPKINS, G. ZONG and H. L. MARCUS (eds), "Development of a Selective Laser Reaction Sintering Workstation", Proceedings of the SFF Symposium, Austin, Texas,Aug. 3–5, 1992.
17. R. M. GERMAN, *J. Metals*, **38**(8) (1986) 26.
18. N. OZKAN, B. A. GLOWACKI, E. A. ROBINSON and P. A. FREEMAN, *J. Mater. Res.* **6**(9) (1991) 1829.
19. B. ROPERS, R. CANET, F. CARMONA and S. FLANDROIS, *Solid State Comm.* **75**(10) (1990) 791.

Received 5 August 1993
and accepted 21 February 1994